Angewandte Zuschriften

Hybrid Materials | Hot Paper

Deutsche Ausgabe: DOI: 10.1002/ange.201502733
Internationale Ausgabe: DOI: 10.1002/anie.201502733

polyMOFs: A Class of Interconvertible Polymer-Metal-Organic-Framework Hybrid Materials**

*Zhenjie Zhang, Ha Thi Hoang Nguyen, Stephen A. Miller, and Seth M. Cohen**

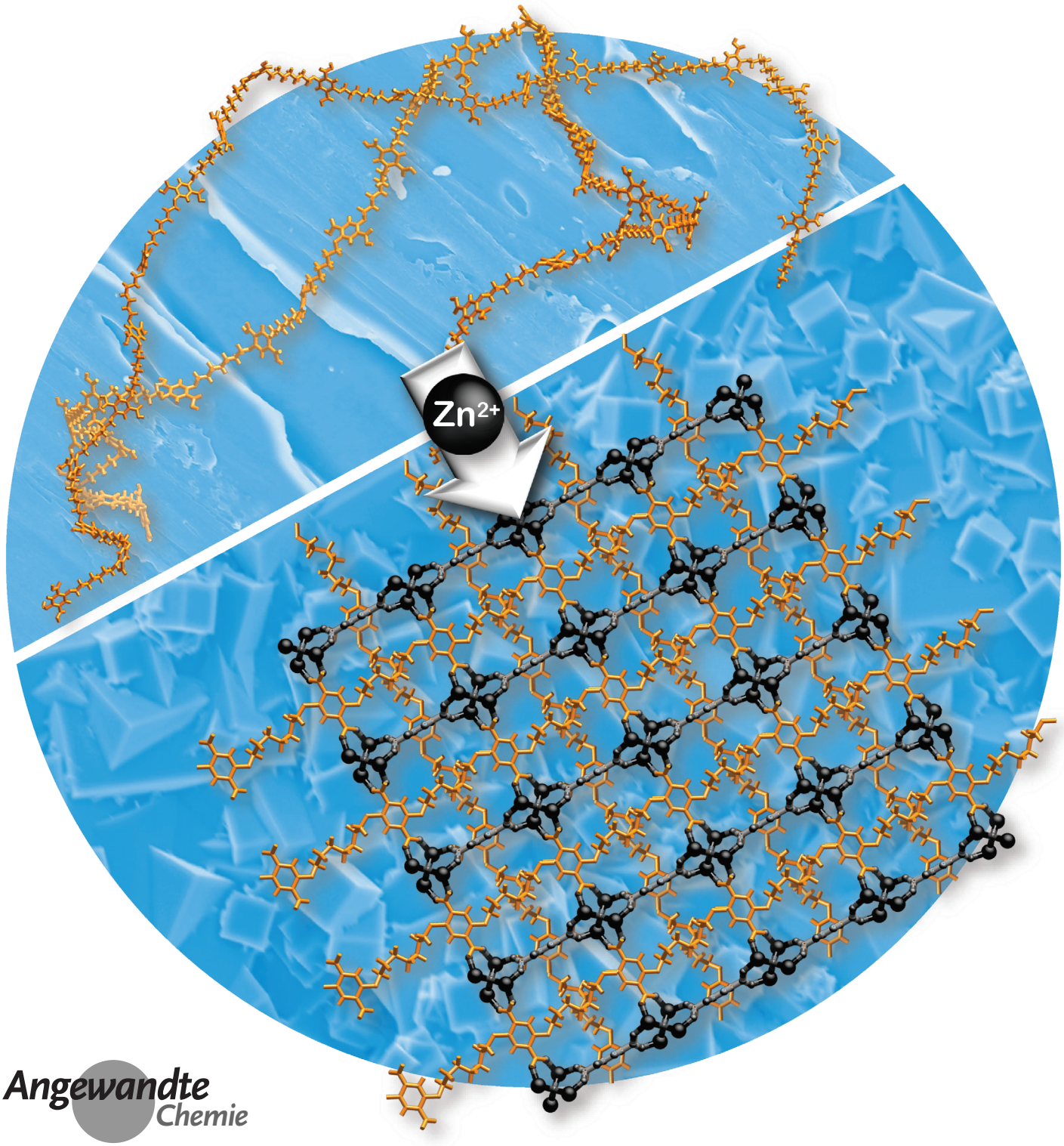

Abstract: *Preparation of porous materials from one-dimensional polymers is challenging because the packing of polymer chains results in a dense, non-porous arrangement. Herein, we demonstrate the remarkable adaptation of an amorphous, linear, non-porous, flexible organic polymer into a three-dimensional, highly porous, crystalline solid, as the organic component of a metal–organic framework (MOF). A polymer with aromatic dicarboxylic acids in the backbone functioned as a polymer ligand upon annealing with Zn^{II}, generating a polymer–metal–organic framework (polyMOF). These materials break the dogma that MOFs must be prepared from small, rigid ligands. Similarly, polyMOFs contradict conventional polymer chemistry by demonstrating that linear and amorphous polymers can be readily coaxed into a highly crystalline, porous, three-dimensional structure by coordination chemistry.*

Porous materials with well-defined size-selective channels and pores have attracted great attention for a wide range of applications: ion exchange, catalysis, gas sorption, and drug delivery.[1] These porous materials include both inorganic and organic materials such as zeolites,[2] metal–organic frameworks (MOFs),[3] and covalent organic frameworks (COFs),[4] among others. MOFs occupy a special place amongst porous materials owing to their extraordinary surface areas (routinely $>2500\ m^2\,g^{-1}$), topological diversity, and high functional tunability.[5] Along with open framework solids, porous one-dimensional polymers have also been developed. In general, the preparation of such porous polymers is challenging because the dense and efficient packing of polymer chains, even for polymers with low crystallinity, affords materials with minimal porosity.[6] To obtain porous organic chain polymers, inflexible and contorted building blocks, which cannot pack efficiently, have been successfully utilized to generate microporosity.[7] For example, McKeown et al. described a novel subclass of microporous polymers (termed polymers of intrinsic microporosity, PIMs), which are amorphous and flexible.[8] The porosity of PIMs can be deformed under external stimulus (for example, light, heat, mechanical stress).[9] However, when compared to traditional porous solids, PIMs have modest surface areas ($<900\ m^2\,g^{-1}$) and their pore size distributions are rather broad (for example, 4–10 Å).[7a] Herein, we report an innovative strategy to compel one-dimensional, non-porous, amorphous polymers into three-dimensional, highly porous, crystalline metal–organic frameworks (MOFs; Scheme 1). The use of organic polymers as a component of MOFs defines a new subclass of porous materials that we term polymer–MOF hybrids (polyMOFs). Such polyMOFs have the potential to harness the advantages

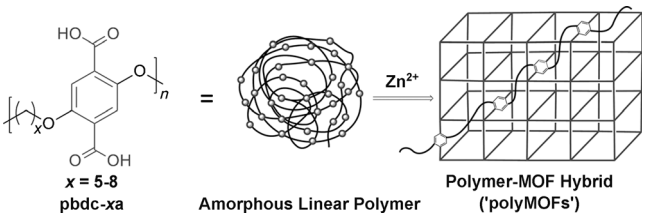

Scheme 1. The strategy described herein to convert a one-dimensional (linear), non-porous, mostly amorphous polymer into a three-dimensional, porous, crystalline polyMOF hybrid material.

of both polymers and MOFs: the porosity, regularity, and crystallinity of MOFs, with the chemical stability, processability, and structural control of polymers. Furthermore, polyMOFs defy conventional wisdom in both MOF and polymer chemistry by showing that a mostly amorphous, non-porous, flexible, one-dimensional polymer can be easily converted into a highly crystalline, porous, rigid, three-dimensional material.

Recently, several groups have demonstrated the cross-linking of MOFs through the organic ligands to form polymeric monoliths.[10] Others have reported the polymerization of molecules inside the channels of MOFs,[11] including the use of photopolymerization methods.[12] These reports described MOF-to-polymer conversions and polymer-within-MOF syntheses, respectively, both of which add to the wealth of MOF–polymer hybrid materials. However, to the best of our knowledge, there is no reported MOF material prepared by bottom-up synthesis that utilizes an amorphous polymer as the organic building block. Indeed, the formation of an organized MOF material from such a disorganized precursor would be considered unlikely based on the current view on the synthesis of MOFs, which would predict the formation of an irregular, amorphous, cross-linked solid from a polymer precursor. Furthermore, from a polymer perspective, a polymer-to-MOF synthesis could be viewed as kinetically and entropically challenging because the unpredictable structure of polymers would seemingly result in chain entanglements and structural irregularities, leading to intractable and amorphous materials. Both chain entanglement and polydispersity are known to hinder the crystallization (self-ordering) of polymers.[13] IRMOF-1 (MOF-5), first described by Yaghi and co-workers in 1999, is a prototypical MOF.[14] Some functional groups, such as halogens, nitro groups, alkyl groups, and others, can be appended to the 1,4-benzenedicarboxylic acid (H_2bdc) ligand struts of IRMOF-1 while maintaining the same structural topology and high porosity (Figure 1).[15] Recently, our group described a novel presynthetic approach to prepare IRMOF-1 derivatives that utilize cross-linked H_2bdc derivatives (Figure 1).[16] It was found that the IRMOF topology can tolerate these linked building blocks resulting in

[*] Dr. Z. Zhang, Prof. Dr. S. M. Cohen
Department of Chemistry and Biochemistry
University of California, San Diego
La Jolla, CA 92093 (USA)
E-mail: scohen@ucsd.edu

H. T. H. Nguyen, Prof. Dr. S. A. Miller
The George and Josephine Butler Laboratory for Polymer Research
Department of Chemistry, University of Florida
Gainesville, FL 32611 (USA)

[**] This work was supported by a grant from the Department of Energy, Office of Basic Energy Sciences, Division of Materials Science and Engineering under Award No. DE-FG02-08ER46519 (S.M.C.) and the National Science Foundation under Award No. CHE-1305794 (S.A.M.)

Supporting information for this article is available on the WWW under http://dx.doi.org/10.1002/anie.201502733.

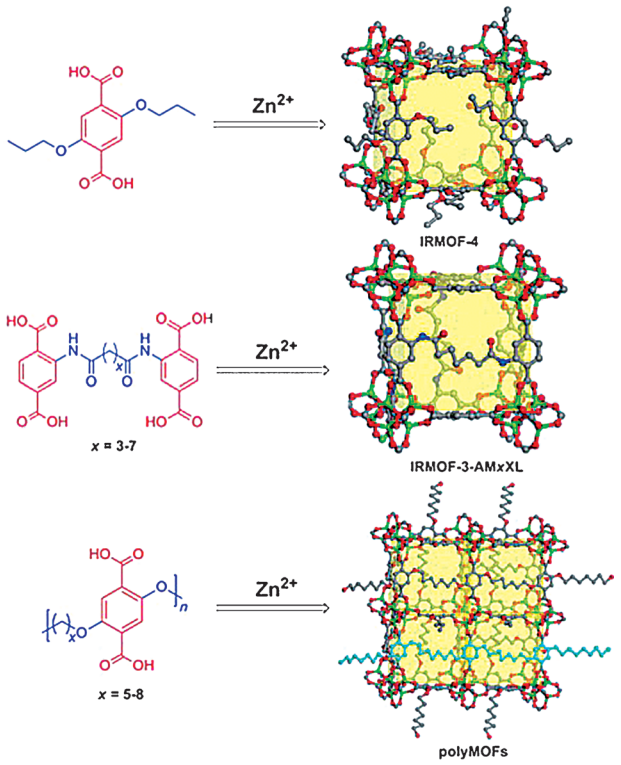

Figure 1. The evolution of IRMOF derivatives constructed from (top to bottom): an H_2bdc ligand derivative, a cross-linked H_2bdc ligand, and a polymeric H_2bdc polymer ligand. One polymer chain segment in the bottom image is highlighted in cyan for clarity. C gray; O red, Zn green.

crystalline IRMOFs. Based on these findings, we sought to explore whether polymers containing repeating H_2bdc units could produce crystalline polyMOFs isostructural to IRMOF-1 (Figure 1).

A series of polymer precursors (termed "polymer ligands") was prepared by step-growth polymerization (Supporting Information, Figure S1).[17] The desired polyethers, containing H_2bdc units as part of the polymer chain backbone (Scheme 1), were obtained in two steps. By using linear dibromoalkanes $Br(CH_2)_xBr$ with different methylene spacers ($x = 5$–8), a series of polyethers having pendent ester functionality (designated as polymeric-bdc-ester, pbdc-*x*e, $x = 5$–8,) was obtained. Hydrolysis of these polymers afforded the corresponding polyethers containing free carboxylic acid H_2bdc units (designated as polymeric-bdc-acid, pbdc-*x*a, $x = 5$–8, Scheme 1). ^{1}H- and ^{13}C NMR spectroscopy showed the high purity of the polymers (Supporting Information, Figures S2–S9). Molecular-weight values were determined by gel permeation chromatography (GPC), which showed that the polymers possessed molecular weights (M_w) ranging from 12500 g mol^{-1} to 17600 g mol^{-1}, with polydispersity index values (PDI) typical of a step-growth polymerization (ranging from about 2.0 to 2.6; Table 1; Supporting Information, Figure S10). Varying the solvent ratio (acetone/DMSO) gave polymers of different molecular weights; for example, lower-molecular-weight pbdc-7a (M_n = 3800 g mol^{-1}, M_w = 8400 g mol^{-1}) was obtained using a higher ratio of acetone to DMSO (see the Supporting Information). All experiments described herein used the higher-molecular-weight polymers, unless specified otherwise (see single-crystal X-ray data below).

Table 1: Thermal and molecular weight data for polymer ligands.

Ligands	T_g [°C]	T_m [°C][a]	M_w [g mol^{-1}]	M_n [g mol^{-1}]	DP[b]	PDI
pbdc-5a	96	229	11700	5900	22	2.0
pbdc-6a	93	226	17600	8400	30	2.1
pbdc-7a	86	211	13500	5900	20	2.3
pbdc-7a[c]	83	206	12000	5200	18	2.3
pbdc-8a	77	202	12500	4700	15	2.6

[a] DSC analysis afforded melting temperatures on the first heating cycle only. No melting was observed in the second cycle. Crystallization was altogether absent. [b] Average degree of polymerization (DP) based on M_n/(F.W.$_{repeat\ unit}$). [c] Recovered pbdc-7a from acid-digested polyMOF.

The glass transition temperature (T_g) of the polymer ligands, determined by differential scanning calorimetry (DSC), revealed a clear trend, showing that the T_g decreases from 96 °C to 77 °C with an increasing number of methylene spacers ($x = 5$–8) in the polymer backbone (Table 1; Supporting Information, Figures S11–S14). This is consistent with more methylene spacers increasing the conformational freedom of the polymer and diluting its polar fraction, resulting in lower T_g values. Similarly, the measured polymer melting temperatures decreased (from 229 to 202 °C) with an increase in the nonpolar methylene spacer length. Note that melting temperatures were found on the first DSC heating cycle only. Measured heats of fusion (ΔH_f = 22 to 44 J g^{-1}) were merely 8 to 15% the value of linear polyethylene (289 J g^{-1}).[18] In subsequent DSC cooling or heating scans, the lack of observable crystallization or melting events punctuates the low crystallinity of these polymers, which was further corroborated by powder X-ray diffraction (PXRD; Figure 2).

A modified version of the typical synthesis for an IRMOF was employed to prepare polyMOF materials. Combining pbdc-*x*a polymer ligands with $Zn(NO_3)_2{\cdot}6H_2O$ in DMF between 60 and 100 °C afforded off-white solids. The topology, structure, and composition of these solids were dependent on which polymer ligand was employed (for

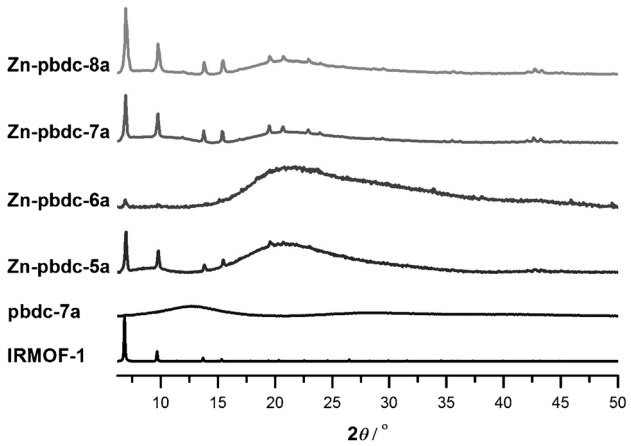

Figure 2. PXRD patterns for pbdc-7a polymer ligand, Zn-pbdc-xa polyMOFs (synthesized at 100 °C), and calculated IRMOF-1.

example, $x = 5–8$) and the temperature of the reaction. At the highest temperature employed (100 °C), the PXRD patterns of all of the products (designated as Zn-pbdc-*x*a) exhibited reflections that showed the formation of an IRMOF-like network (Figure 2). All of the PXRD patterns also showed a broad peak centered at $2\theta \approx 22°$, indicating the existence of an amorphous phase, the abundance of which was dependent on the polymer composition (for example, $x = 5–8$). Zn-pbdc-8a and Zn-pbdc-7a had very little amorphous phase, as gauged by PXRD (and scanning electron microscopy, see below), while Zn-pbdc-6a and Zn-pbdc-5a showed a greater amorphous component. Zn-pbdc-6a showed a particularly large amorphous component and only a small IRMOF component; why this polymer behaves substantially differently from the others is not clear at this time.

The morphology and particle size of the resulting materials was determined by SEM. Unlike typical IRMOF materials (for example, IRMOF-1), which form large, macroscopic crystals, the particle size of the polyMOF samples formed at 100 °C was on the order of 1–10 μm. As shown in Figure 3, the majority of Zn-pbdc-5a particles possess a spherical shape, with only a small number of cubic particles observed. Consistent with the PXRD results (Figure 2), the cubic morphology is typical of IRMOF derivatives, while the spherical particles suggest an amorphous structure.[19] Energy-dispersive X-ray spectroscopy (EDX) revealed the presence of Zn^{II} in the spheres (Supporting Information, Figure S15), indicating the spheres are comprised of coordination complexes of Zn^{II} and pbdc-5a, but lack a highly ordered arrangement. Similar to Zn-pbdc-5a, Zn-pbdc-6a also displays mixed phases when formed at 100 °C with irregularly shaped solids (Figure 3), consistent with the PXRD pattern. In contrast, Zn-pbdc-7a and Zn-pbdc-8a exhibit very different morphologies. Although both spherical and cubic particles are observed (Figure 3), closer examination shows that the spherical solids are intergrown crystalline superstructures with regular facets.[20] We interpret the polycrystalline, spherical superstructures of Zn-pbdc-7a and Zn-pbdc-8a as the result of many individual crystals growing together and partially sharing polymer ligands. This most likely results from the formation of multiple nucleation sites for IRMOF growth on individual polymer ligand chains and intergrowth of polymer ligand chains during coordination to Zn^{II}.

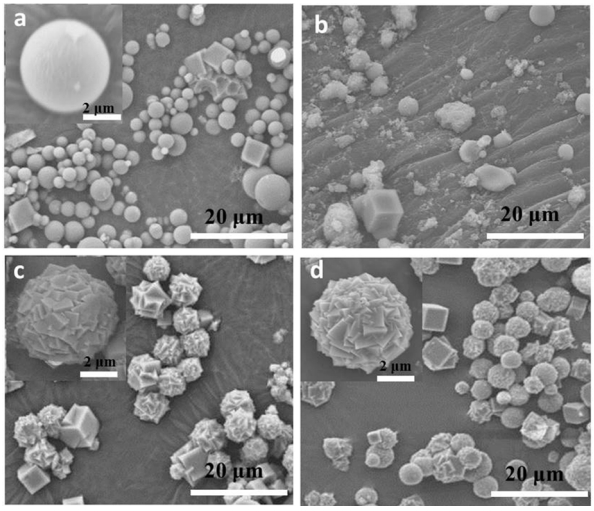

Figure 3. SEM images of Zn-pbdc-*x*a particles prepared at 100 °C: a) Zn-pbdc-5a; b) Zn-pbdc-6a; c) Zn-pbdc-7a; and d) Zn-pbdc-8a.

To exclude the possibility that only oligomers or smaller molecular weight species were responsible for MOF formation, a representative reaction with pbdc-7a was monitored by ^{1}H NMR spectroscopy in [D_7]DMF. ^{1}H NMR data revealed the complete consumption of the polymer ligands (Supporting Information, Figures S16 and S17). The possibility of polymer ligand degradation during the synthesis process was also excluded. Zn-pbdc-7a was digested in concentrated aqueous D_2O/DCl and then precipitated by adding excess water. GPC and ^{1}H NMR data confirmed that the recovered polymer ligands remained intact (Table 1; Figure S18).

Although the cubic single crystals in as-synthesized Zn-pbdc-*x*a powders were too small for routine single-crystal X-ray diffraction (XRD), larger cubic crystals (ca. 20 μm) suitable for XRD could be prepared from lower molecular weight pbdc-7a ($M_n = 3800\ g\,mol^{-1}$; see above). XRD data confirmed the IRMOF network of these materials. The position of the heptamethylene linkers between the bdc^{2-} units was not resolved, which is most likely because these linkers are disordered with respect to conformation and occupancy. This is consistent with our earlier reports on cross-linked MOFs,[16a] where linkers were also not observed in the XRD analysis.

Further study revealed that the morphology of polyMOFs could be controlled using different polymer ligands and by changing the reaction temperature. At a lower temperature of 80 °C, rather than forming spheroidal structures, Zn-pbdc-7a and Zn-pbdc-8a produced crystalline films, showing an intergrown network of crystallites (Figure 4). The films were about 20 μm thick (Supporting Information, Figure S19). Such films may prove useful for small molecule and gas separations, and these investigations are in progress.

The incorporated alkyl chains of the polymer ligands would be expected to increase the hydrophobicity of the resulting hybrid material. Contact angle measurements with water show that the polymer ligands pbdc-5a and pbdc-6a are hydrophilic, while pbdc-7a is partially hydrophobic (initial contact angle ca. 89°, followed by liquid absorption after about 1 min) and pbdc-8a is hydrophobic with a contact angle

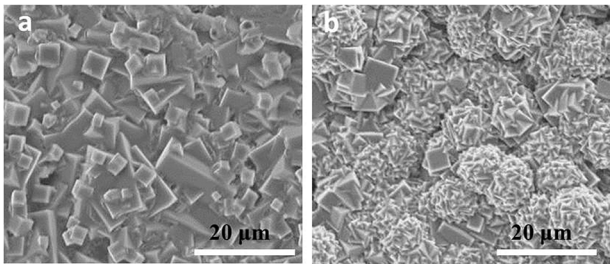

Figure 4. The film morphology of Zn-pbdc-xa prepared at 80 °C: a) Zn-pbdc-7a; b) Zn-pbdc-8a.

of $102 \pm 2°$ (with no change over several minutes). A measurement of contact angles for the polyMOF materials was performed revealing that polyMOFs exhibit the same trend as their corresponding polymer ligands: Zn-pbdc-5a and Zn-pbdc-6a are hydrophilic; Zn-pbdc-7a is partially hydrophobic with initial contact angle of about 92°; and Zn-pbdc-8a is hydrophobic with a contact angle of $112 \pm 2°$. The increased hydrophobicity was examined with respect to the stability of polyMOFs compared to other IRMOF materials. For example, the PXRD pattern of IRMOF-1 disappears upon exposure to ambient air for 1 day,[21] eventually transforming to a PXRD pattern consistent with MOF-69c (Supporting Information, Figure S20).[22] In contrast, the first two characteristic PXRD peaks for Zn-pbdc-8a shift only slightly to higher angle upon exposure to ambient air for 1 day and showed no significant intensity decrease even after 3 days in air (Supporting Information, Figure S21). Furthermore, the native Zn-pbdc-8a can be regenerated by simply immersing the crystals in DMF at 60 °C for 1 hour, as verified by PXRD. The regenerated polyMOF retains the original morphology (Supporting Information, Figure S22), suggesting neither dissolution nor reformation of the crystallites. By comparison, IRMOF-1 cannot be regenerated via the same procedure after decomposition in air (Figure S20).

Just as the polyMOF can inherit the hydrophobicity of the polymer, it was anticipated that the polyMOF would possess the porosity of the parent IRMOF structure. N_2 and CO_2 sorption were collected on several samples. The pbdc-*x*a polymer ligands are non-porous, which is presumably due to their amorphous structure and tight packing of polymer chains. In contrast, polyMOF samples Zn-pbdc-5a, Zn-pbdc-7a, and Zn-pbdc-8a exhibit typical type I isotherms at 77 K, indicating a uniform microporous structure (Figure 5). Calculations based on N_2 adsorption isotherms reveal that Zn-pbdc-5a, Zn-pbdc-7a, and Zn-pbdc-8a possess Brunauer–Emmett–Teller (BET) surface areas of 232 ± 15, 1104 ± 28, and $856 \pm 16\ m^2 g^{-1}$, respectively. Interestingly, Zn-pbdc-6a exhibits a distinctive type II sorption isotherm, indicating the existence of macroporosity, likely generated by particle packing. As such, Zn-pbdc-6a displays a low BET surface area of about $70\ m^2 g^{-1}$. The relatively low surface areas of Zn-pbdc-5a and Zn-pbdc-6a are consistent with the PXRD and SEM data, and suggest that these two polyMOFs are largely amorphous, unlike Zn-pbdc-7a and Zn-pbdc-8a.

To investigate any differences between IRMOFs and polyMOFs, two dimeric H_2bdc ligands linked by a single heptamethylene or octamethylene spacer, L1 and L2 (Supporting Information, Figure S1), were synthesized by reported methods.[23] Using these dimeric ligands, model IRMOFs were prepared, IRMOF-L1 and IRMOF-L2, which contain the same linker length as in Zn-pbdc-7a and Zn-pbdc-8a, respectively, but are not polymeric in nature. IRMOF-L1 and IRMOF-L2 possess IRMOF structures as verified by PXRD (Supporting Information, Figure S23). IRMOF-1, IRMOF-L1, and IRMOF-L2 exhibit BET surface areas of 2963 ± 30, 1883 ± 17, and $1817 \pm 16\ m^2 g^{-1}$, respectively. Although polyMOFs exhibited lower surface areas than IRMOF-1, IRMOF-L1, and IRMOF-L2, the polyMOFs were found take up more CO_2 (Figure 5b; Supporting Information, Figure S24). Zn-pbdc-8a, Zn-pbdc-7a, IRMOF-L1, IRMOF-L2, and IRMOF-1 can uptake 41, 49, 30, 35, and $20\ cm^3 g^{-1}$ of CO_2 at 1 atm and 298 K, respectively. This observation suggests that the isosteric heat (Q_{st}) of CO_2 adsorption of Zn-pbdc-8a and Zn-pbdc-7a is higher than those of IRMOF-1, IRMOF-L1, and IRMOF-L2. Virial equation calculations[24] based on CO_2 isotherms collected at 273 and 298 K revealed that initial Q_{st} values for Zn-pbdc-8a and Zn-pbdc-7a are 19.9 and 20.6 kJ mol^{-1} respectively, which are higher than IRMOF-1 (14.2 kJ mol^{-1})[24] and its derivatives, IRMOF-L1 (17.8 kJ mol^{-1}) and IRMOF-L2 (15.4 kJ mol^{-1}; Supporting Information, Figure S25). The pore size distribution was calculated by density functional theory (DFT) methods from the N_2 sorption isotherms (Supporting Information, Figure S26). IRMOF-1 possesses the largest pore size (ca. 13 Å), IRMOF-L1 and IRMOF-L2 possess medium pore size (ca. 11 Å), and Zn-pbdc-7a and Zn-pbdc-8a exhibited the smallest pore sizes (ca. 7 Å and 9 Å). The reduction in pore size most certainly originates from the incorporation of polymer chains in the Zn-pbdc-xa frameworks, making the pore widths of the polyMOFs smaller than those of IRMOF-1, IRMOF-L1, and IRMOF-L2. The smaller

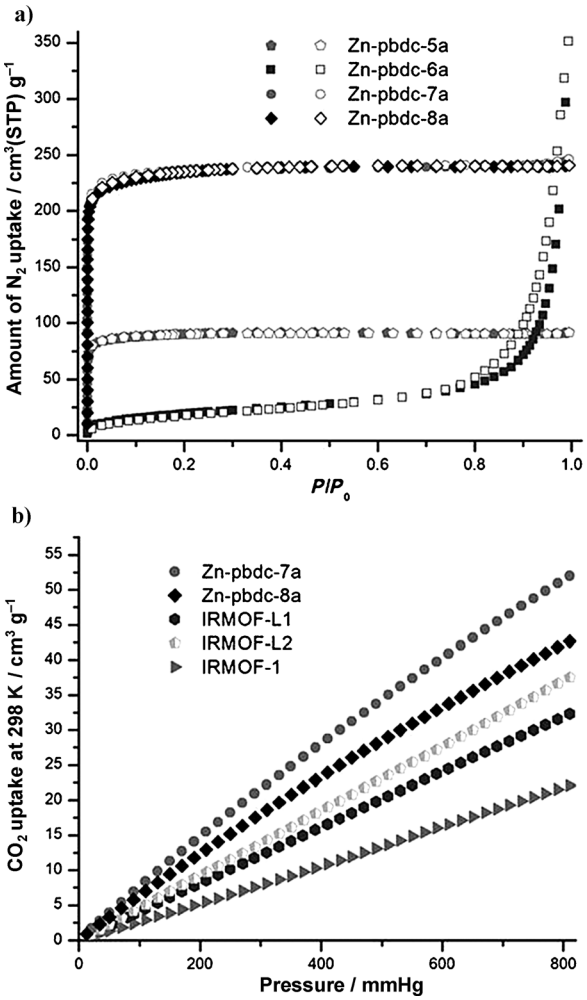

Figure 5. a) N_2 sorption isotherms for polyMOFs; b) CO_2 adsorption isotherms at 298 K.

pore sizes may explain the stronger interactions between CO_2 and the polyMOFs, as a decrease in Q_{st} for CO_2 has been shown to correlate with increases in pore size.[25]

In summary, we report a strategy to generate porosity from non-porous, one-dimensional, amorphous polymeric materials by their transformation into crystalline polyMOF materials by a solvothermal synthesis (annealing) with Zn^{II} cations. A series of non-porous polymer ligands with terephthalate moieties was designed and prepared that upon hydrothermal reaction with Zn^{II} cations, forms polycrystalline, hybrid materials with IRMOF networks. PXRD, SEM, and gas-sorption data confirm these materials are crystalline, porous, and share the same structure type as IRMOF-1. The incorporation of polymers into MOFs was shown to harness advantages of both materials, including hydrophobicity and permanent porosity. Furthermore, by selecting certain polymer ligands at specific annealing temperatures, polyMOF materials exhibit morphologies ranging from spherical superstructures to crystalline films. The formation of polyMOFs from linear organic polymers defies conventional wisdom in both polymer and MOFs fields and opens up the opportunity for the discovery in a new class of materials with emergent properties.

Keywords: gas sorption · hybrid materials · hydrophobicity · metal–organic frameworks · polymers

How to cite: *Angew. Chem. Int. Ed.* **2015**, *54*, 6152–6157
Angew. Chem. **2015**, *127*, 6250–6255

[1] a) D. W. Bruce, D. O'Hare, R. I. Walton, *Porous Materials*, Wiley, Chichester, **2011**; b) M. E. Davis, *Nature* **2002**, *417*, 813–821.
[2] S. M. Kuznicki, *Zeolite Molecular Sieves: Structure Chemistry and Use*, Wiley, Hoboken, **2013**.
[3] a) L. R. MacGillivray, *Metal-Organic Frameworks: Design and Application*, Wiley, Hoboken, **2010**; b) H.-C. Zhou, S. Kitagawa, *Chem. Soc. Rev.* **2014**, *43*, 5415–5418.
[4] S.-Y. Ding, W. Wang, *Chem. Soc. Rev.* **2013**, *42*, 548–568.
[5] a) H. Deng, S. Grunder, K. E. Cordova, C. Valente, H. Furukawa, M. Hmadeh, F. Gándara, A. C. Whalley, Z. Liu, S. Asahina, H. Kazumori, M. O'Keeffe, O. Terasaki, J. F. Stoddart, O. M. Yaghi, *Science* **2012**, *336*, 1018–1023; b) D. Feng, T.-F. Liu, J. Su, M. Bosch, Z. Wei, W. Wan, D. Yuan, Y.-P. Chen, X. Wang, K. Wang, X. Lian, Z.-Y. Gu, J. Park, X. Zou, H.-C. Zhou, *Nat. Commun.* **2015**, *6*, 5979; c) H. Furukawa, N. Ko, Y. B. Go, N. Aratani, S. B. Choi, E. Choi, A. O. Yazaydin, R. Q. Snurr, M. O'Keeffe, J. Kim, O. M. Yaghi, *Science* **2010**, *329*, 424–428.
[6] J. D. Dunitz, G. Filippini, A. Gavezzotti, *Tetrahedron* **2000**, *56*, 6595–6601.
[7] a) N. B. McKeown, *ISRN Mater. Sci.* **2012**, *2012*, 16; b) N. B. McKeown, P. M. Budd, *Chem. Soc. Rev.* **2006**, *35*, 675–683.
[8] a) P. M. Budd, B. S. Ghanem, S. Makhseed, N. B. McKeown, K. J. Msayib, C. E. Tattershall, *Chem. Commun.* **2004**, 230–231; b) M. Carta, R. Malpass-Evans, M. Matthew Croad, Y. Rogan, J. C. Jansen, P. Bernardo, F. Bazzarelli, N. B. McKeown, *Science* **2013**, *339*, 303–307.
[9] Q. Song, S. Cao, R. H. Pritchard, B. Ghalei, S. A. Al-Muhtaseb, E. M. Terentjev, A. K. Cheetham, E. Sivaniah, *Nat. Commun.* **2014**, *5*, 4813.
[10] a) Y. Furukawa, T. Ishiwata, K. Sugikawa, K. Kokado, K. Sada, *Angew. Chem. Int. Ed.* **2012**, *51*, 10566–10569; *Angew. Chem.* **2012**, *124*, 10718–10721; b) T. Ishiwata, Y. Furukawa, K. Sugikawa, K. Kokado, K. Sada, *J. Am. Chem. Soc.* **2013**, *135*, 5427–5432; c) M. Tsotsalas, J. Liu, B. Tettmann, S. Grosjean, A. Shahnas, Z. Wang, C. Azucena, M. Addicoat, T. Heine, J. Lahann, J. Overhage, S. Bräse, H. Gliemann, C. Wöll, *J. Am. Chem. Soc.* **2014**, *136*, 8–11.
[11] G. Distefano, H. Suzuki, M. Tsujimoto, S. Isoda, S. Bracco, A. Comotti, P. Sozzani, T. Uemura, S. Kitagawa, *Nat. Chem.* **2013**, *5*, 335–341.
[12] I.-H. Park, A. Chanthapally, Z. Zhang, S. S. Lee, M. J. Zaworotko, J. J. Vittal, *Angew. Chem. Int. Ed.* **2014**, *53*, 414–419; *Angew. Chem.* **2014**, *126*, 424–429.
[13] a) G. Odian, *Principles of Polymerization*, Wiley, Hoboken, **2004**; b) L. H. Sperling, *Introduction to Physical Polymer Science*, Wiley, Hoboken, **2006**.
[14] H. Li, M. Eddaoudi, M. O'Keeffe, O. M. Yaghi, *Nature* **1999**, *402*, 276–279.
[15] H. Deng, C. J. Doonan, H. Furukawa, R. B. Ferreira, J. Towne, C. B. Knobler, B. Wang, O. M. Yaghi, *Science* **2010**, *327*, 846–850.
[16] a) C. A. Allen, J. A. Boissonnault, J. Cirera, R. Gulland, F. Paesani, S. M. Cohen, *Chem. Commun.* **2013**, *49*, 3200–3202; b) C. A. Allen, S. M. Cohen, *Inorg. Chem.* **2014**, *53*, 7014–7019.
[17] D. A. Schlüter, C. Hawker, J. Sakamoto, *Synthesis of Polymers: New Structures and Methods*, Wiley, Hoboken, **2012**.
[18] L. Mandelkern, A. L. Allou, M. R. Gopalan, *J. Phys. Chem.* **1968**, *72*, 309–318.
[19] Y. Zhou, J. Zhang, G. Su, J. Li, *Sci. Rep.* **2014**, *4*, 6250.
[20] a) A. Carné-Sánchez, I. Imaz, M. Cano-Sarabia, D. Maspoch, *Nat. Chem.* **2013**, *5*, 203–211; b) M. Pang, A. J. Cairns, Y. Liu, Y. Belmabkhout, H. C. Zeng, M. Eddaoudi, *J. Am. Chem. Soc.* **2013**, *135*, 10234–10237.
[21] J. G. Nguyen, S. M. Cohen, *J. Am. Chem. Soc.* **2010**, *132*, 4560–4561.
[22] S. S. Kaye, A. Dailly, O. M. Yaghi, J. R. Long, *J. Am. Chem. Soc.* **2007**, *129*, 14176–14177.
[23] S.-M. Huh, J. I. Jin, M.-F. Achard, F. Hardouin, *Liquid Crystals* **1998**, *25*, 285–293.
[24] K. Sumida, D. L. Rogow, J. A. Mason, T. M. McDonald, E. D. Bloch, Z. R. Herm, T.-H. Bae, J. R. Long, *Chem. Rev.* **2012**, *112*, 724–781.
[25] P. Nugent, Y. Belmabkhout, S. D. Burd, A. J. Cairns, R. Luebke, K. Forrest, T. Pham, S. Ma, B. Space, L. Wojtas, M. Eddaoudi, M. J. Zaworotko, *Nature* **2013**, *495*, 80–84.

Received: March 24, 2015
Published online: April 29, 2015

